Supporting information

Core-shell Nanospheres Enabling Ultralow Friction Polymer Nanocomposites with Superior Mechanical Properties

Lin Zhang, Yilong Ren, Shiguang Peng, Dan Guo, Shizhu Wen, Jianbin Luo, Guoxin Xie*

State Key Laboratory of Tribology, Department of Mechanical Engineering, Tsinghua University, Beijing 100084, China

*Corresponding author: xgx2014@tsinghua.edu.cn (Guoxin Xie)

I. PTFE@PMMA core-shell nanospheres

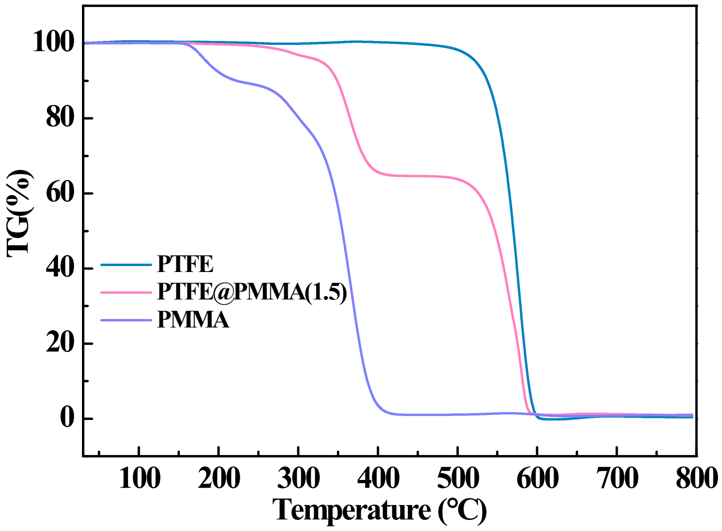

Figure S1. TG curves at 10 ºC /min heating rate for samples.

The thermal stability of PMMA, PTFE and PTFE@PMMA(1.5) were evaluated by TG analysis from 25 to 800 ºC at a heating rate of 10 ºC /min under nitrogen atmosphere and the results were presented in Figure S1. From TG profiles, two main weightless steps centered at 365 and 560 ºC were observed, which were clearly assignable to PMMA and PTFE decomposition respectively. For pure PMMA and PTFE@PMMA(1.5) samples, besides the large weight loss peak of PMMA at 365 ºC, there are another two small weight loss steps at 175 and 290 ºC, which were assignable to small molecule oligomer in the synthesized samples.

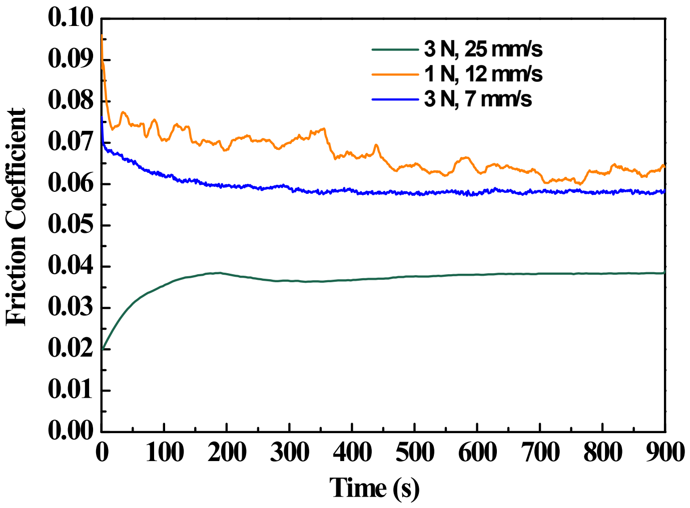

Figure S2. Frictional properties of PTFE@PMMA(1.5) nanocomposite under different loads and sliding speeds.

The friction coefficient of PTFE@PMMA(1.5) sample was tested under different loads and sliding speeds. As shown in Figure S2, the PTFE@PMMA(1.5) nanocomposite exhibited a relative high friction coefficient (~0.07) at a load of 1 N and a sliding speed of 12 mm/s, and properly increasing the load and the sliding speed could effectively promote the lubrication properties.

II. PTFE@PS core-shell nanospheres

Materials Preparation. The PTFE@PS core-shell nanospheres were synthesized by seed emulsion polymerization. The entire polymerization procedure was carried out under nitrogen atmosphere and a 1 L four-neck jacketed reactor equipped with a condenser, a mechanical stirrer and inlets for nitrogen and monomer was adopted for chemical reaction. Under a stirring rate of 300 rpm and room temperature, 20 mL PTFE latex was introduced into the reactor containing 500 mL deionized water. The mixture was heated to 80 ºC and then styrene was added. After 15 min, a potassium persulfate aqueous solution was added and the mixture was reacted for 12 h. The product was purified by repeated dialyses then dried at 80 ºC for 5 h. A series of core-shell nanospheres were obtained by changing the amount of styrene. The synthesized core-shell nanospheres were adopted as the structural units to form bulk nanocomposites by compression molding. The obtained sample is labeled as PTFE@PS (x), in which x indicates the core-shell mass ratio, which was obtained by thermogravimetric analysis (TGA). The pure PS sample was synthesized under the same conditions and pure PTFE was obtained from PTFE latex used in the emulsion polymerization process. For comparison, composite materials (labelled as PTFE/PS (0.3)) with a mass ratio of PTFE to PS of

0.3 were prepared by the ball milling method. All the prepared powders were loosened before being put in a mold and subjected to cold compaction at 25 MPa for 20 min, followed by sintering at 160 ºC for 60 min.

Characterization. Scanning electron microscopy (SEM, HITACHI UHR FE-SEM SU8220) transmission electron microscopy (TEM, JEM2010) were used to determine the morphologies of the samples. The compressive strength and compressive creep properties of the samples were analyzed with an electronic universal material testing machine. During the compressive creep tests, the constant loading pressure was 8 MPa, and the loading time was 20 min. The friction tests of the nanocomposites were carried out with a universal ball-on-disk microtribometer (UMT-3, CETR, USA) under dry sliding conditions. GCr15 bearing steel balls of Φ4.6 mm in diameter with a surface roughness of 5 nm (as provided by the supplier) were used as the counterface. The friction tests were carried out at a reciprocating speed of 12 mm/s and under applied loads of 1, 3 and 4 N for 15 min.

Results and Discussion

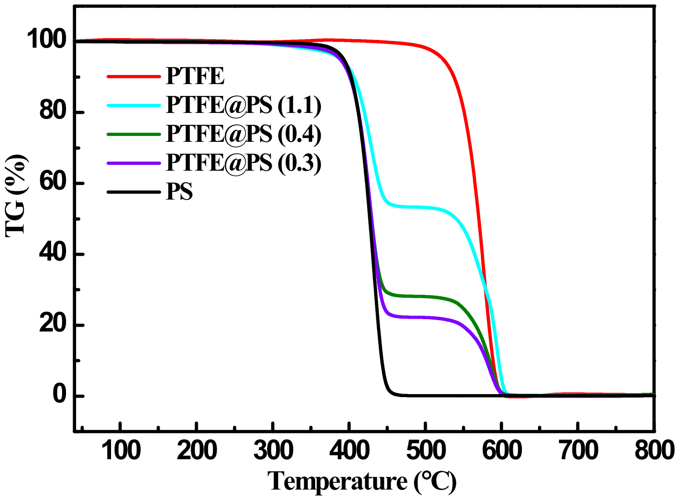

Figure S3. TGA curves of different samples at a heating rate of 10 ℃ /min.

Figure S3 shows the TGA curves of different samples at a heating rate of 10 ºC/min. The weight losses at 360 and 500 °C can be assignable to the PS and PTFE decomposition, respectively. According to the different decomposition temperatures of pure PS and PTFE samples, the compositions of the PTFE@PS(x) core-shell nanospheres were calculated and the 'x' were 1.1, 0.4 and 0.3, respectively. It is evident that the PS weight loss increased proportionally to the initially added styrene.

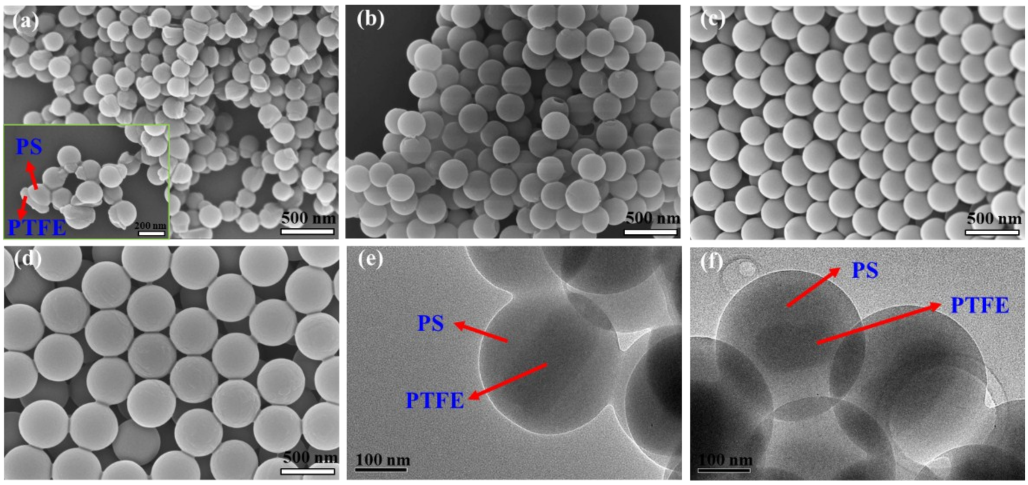

Figure S4. SEM micrographs of the PTFE@PS (1.1) (a), PTFE@PS (0.4) (b), PTFE@PS (0.3) (c) and PS nanospheres (d). TEM micrographs of the PTFE@PS (0.4) (e), PTFE@PS (0.3) (f).

The SEM micrographs of PTFE@PS and PS nanoparticles are shown in Figure S4 (a)-(d). Rod-like PTFE latices were used in this work and the synthesized PTFE@PS and PS particles were spherical structures with relative homogeneous particle sizes. The average sizes of PTFE@PS (1.1), PTFE@PS (0.4), PTFE@PS (0.3) and PS nanospheres were 200, 280, 304, and 452 nm, respectively, and they were calculated from the statistical SEM data over 100 nanoparticles. It is noteworthy that when the core-shell mass ratio was relatively large, that was, the amount of monomer styrene added in the synthesis process was less, the polystyrene obtained by polymerization cannot completely encapsulate PTFE core, resulting in the partial exposure of PTFE core, as shown in the inset to Figure S4 (a). As shown in Figure S4 (b), when the core-shell mass ratio was reduced from 1.1 to 0.4, the PTFE core was completely encapsulated, and however there were still a few nanospheres with structural defects. With the further decreasing core-shell mass ratio, complete and uniformly distributed nanospheres were synthesized, as shown in Figure S4 (c). TEM was used for further characterize the microstructures of the synthesized nanospheres. The apparent core-shell structures of the nanospheres in Figure S4 (e) and (f) indicate PTFE particles were employed as the seeds in the emulsifier-free styrene emulsion polymerization to obtain the PTFE@PS core-shell particles.

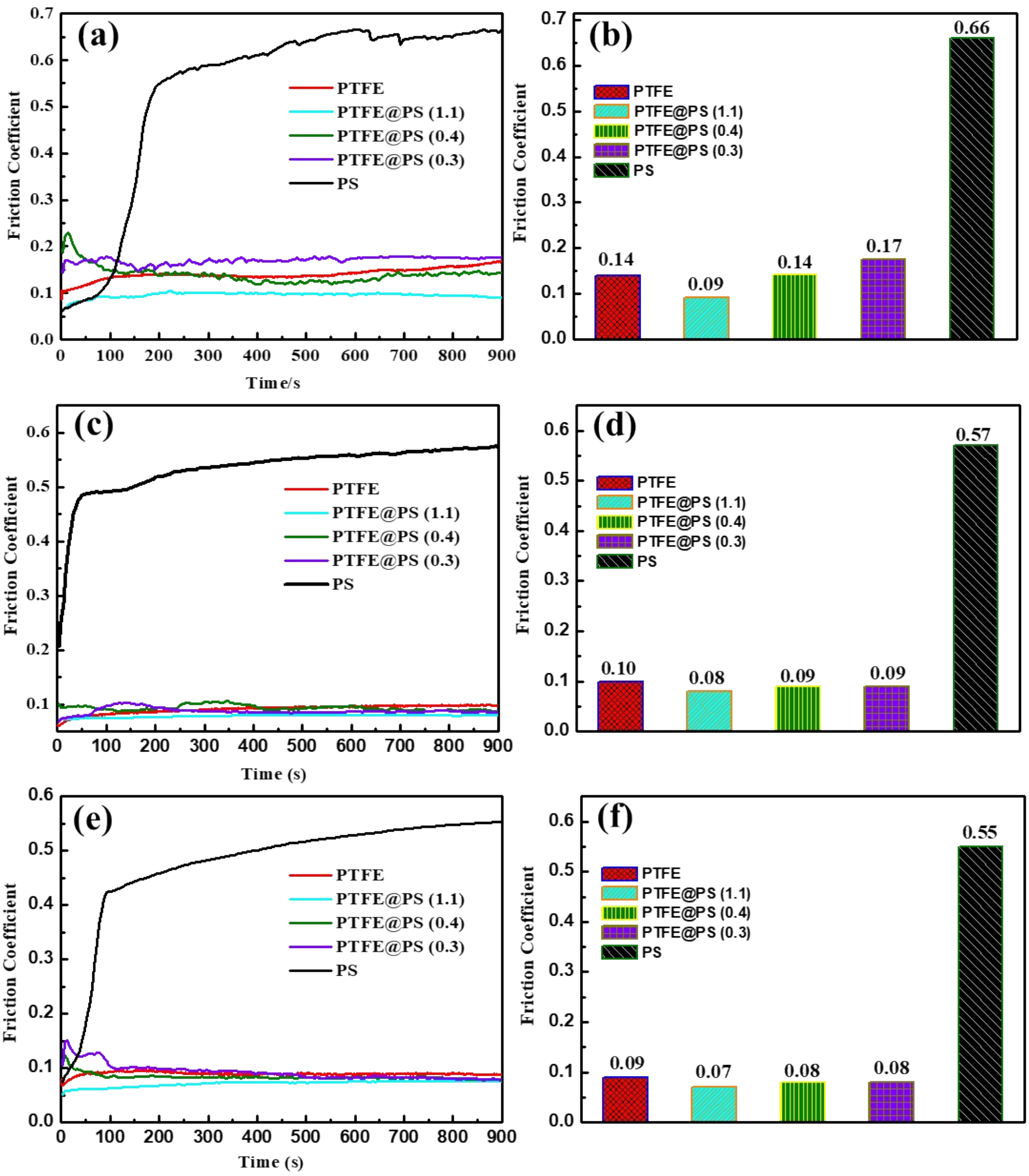

Figure S5. Friction coefficients of the samples at different loads: 1 N (a) and (b); 3 N (c) and (d); 4 N (e) and (f).

The frictional properties of pure PTFE, pure PS and PTFE@PS nanocomposites were investigated. Figure S5 presents the friction coefficients of the nanocomposites under different loads. In Figure S5 (a) and (b), the friction coefficient of the pure PS sample was relatively low in the beginning, and as time progressed, the friction coefficient increased to 0.66 gradually. The pure PTFE exhibited rather stable friction coefficient (around 0.14) during the whole test and the friction coefficient recorded for PTFE@PS (1.1) composite was around 0.09, which was much lower than those for pure PS and PTFE. Nevertheless, with the decrease of the core-shell mass ratio, the content of shell material with poor lubricity increased, resulting in slight reduction of the lubrication performance of the core-shell nanocomposite. The frictional properties of the samples were further investigated by increasing the load to 3 and 4 N. As shown in Figure S5 (c)-(f), the friction coefficient of all samples decreases with the load increase, probably owing to the formation of a stable transfer film under the high load. With the increase of the load, the PTFE@PS core-shell nanocomposites exhibited excellent lubrication properties, which were not significantly affected by the core-shell mass ratio. It was confirmed that the load increase made the core-shell nanoparticles easier to destroy, giving rise to the exposure of the PTFE core, which mainly acted as the lubrication role in the core-shell composites.

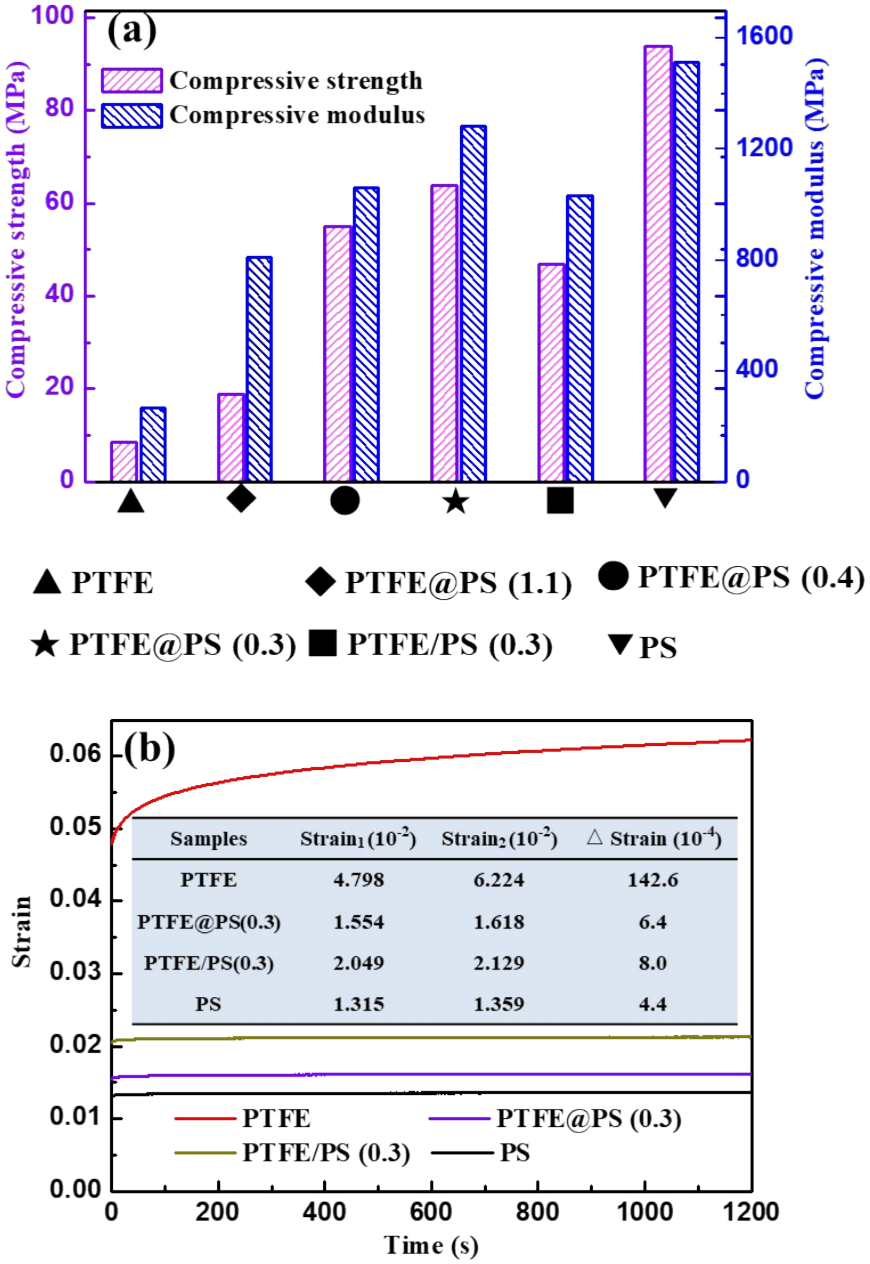

Samples	$Strain_1 (10^{-2})$	$Strain_2 (10^{-2})$	△ Strain (10^{-4})
PTFE	4.798	6.224	142.6
PTFE@PS(0.3)	1.554	1.618	6.4
PTFE/PS(0.3)	2.049	2.129	8.0
PS	1.315	1.359	4.4

Figure S6. The compression (a) and the creep (b) test results of the samples.

The compressive strength is one vital mechanical property that can reflect the ability of a material to resist compression and abrasion. Figure S6 (a) shows the experimentally measured compressive strengths and moduli of the nanocomposites. The compressive strength and modulus of pure PTFE are 8.6 and 269 MPa, respectively. In contrast, the compressive strengths and moduli of the nanocomposites on the basis of core-shell nanospheres are greatly improved, basically being consistent with the results of the PTFE@PMMA nanocomposite in the main text. Representatively, the compressive strength and modulus of the PTFE@PS (0.3) core-shell composite are 64 and 1285 MPa, respectively, which are much higher than those of traditionally mechanical mixing sample, i.e., PTFE/PS (0.3) composite. Creep resistance is another significant parameter for evaluating the stability and reliability of a material. PTFE tends to suffer severe creep under external loading, which seriously affects the safe operation of equipments. As shown in Figure S6 (b), in the process of the rapid increase of the load to 8 MPa, PTFE encountered a large strain, which increased gradually during the holding process. When PTFE and PS were compounded by the core-shell structure, the creep resistance of the nanocomposite was greatly enhanced. It was noteworthy that the creep resistance of PTFE@PS (0.3) core-shell nanocomposite was much better than that of the traditionally mechanical mixing sample, i.e., PTFE/PS (0.3) composite.